Dalton
Transactions

Cite this: *Dalton Trans.*, 2011, **40**, 8643

www.rsc.org/dalton

PAPER

Binuclear half-metallocene chromium(III) complexes mediated ethylene polymerization with alkylaluminium as cocatalyst†

Tieqi Xu,* Yu Pan and Xiao-Bing Lu*

Received 30th April 2011, Accepted 21st June 2011
DOI: 10.1039/c1dt10803d

Binuclear half-metallocene chromium complexes $\{Cp^*[3\text{-}(CH{=}NR)\text{-}2\text{-}O\text{-}C_{10}H_5]CrCl\}_2$ [$Cp^* = C_5Me_5$; R = ^{i}Pr (**1**), Ph (**2**), 2,6-^{i}Pr$_2$C$_6$H$_3$ (**3**)] based on 1,1′-binaphthyl ligands, as well as their mononuclear analogues $Cp^*[3\text{-}(CH{=}NR)\text{-}2'\text{-}R'\text{-}2\text{-}O\text{-}C_{20}H_{11}]CrCl$ [R = ^{i}Pr, R′ = ^{n}BuO (**4**), R = Ph, R′ = ^{n}BuO (**5**), R = 2,6-^{i}Pr$_2$C$_6$H$_3$, R′ = ^{n}BuO (**6**), R = ^{i}Pr, R′ = H (**7**)], were synthesized and characterized by mass spectrometry, elemental analysis, magnetic measurement, and UV-vis spectroscopy. The molecular structures of complexes **1**, **3**, **5** and **6** were further confirmed by single-crystal X-ray crystallographic analysis. When activated with a small amount of $AlMe_3$, these binuclear complexes exhibited higher activities in catalyzing ethylene polymerization in comparison with their mononuclear analogues, affording high molecular weight polymers with unimodal molecular weight distributions. The highest activity up to 2.87×10^6 g PE (mol Cr)$^{-1}$ h^{-1} was achieved in the catalyst system of complex **3** bearing a bulky 2,6-^{i}Pr$_2$C$_6$H$_3$ group on the imine nitrogen atom in the presence of 25 equiv. $AlMe_3$ as activator at 20 °C. ^{13}C NMR analysis indicates the resultant polymers are linear and no evidence on branch was found.

Introduction

Over the past few decades, metallocene type catalysts for olefin polymerization have attracted considerable attention, since they can provide a variety of polyolefin products with high performance, such as isotactic polypropylene,[1] syndiotactic polypropylene,[2] linear low-density polyethylene,[3] syndiotactic polystyrene.[4] One of the most important catalysts is half-metallocene chromium(III) complexes, which are considered to be very promising catalysts for olefin polymerization.[5–7] Particularly, these half-metallocene chromium(III) catalysts usually exhibit good activity with no need for large amounts of MAO (methylaluminoxane) or expensive fluorinated borate such as $[Ph_3C]^+[B(C_6F_5)_4]^-$ as cocatalyst or activator. It is beneficial to significantly lower the ash content (Al_2O_3) of the polymers. Unfortunately, only very limited half-metallocene chromium(III) complexes have been synthesized, possibly owing to their poor characteristics with regard to the paramagnetism. Complexes $[Cp^*CrL_2R]^+A^-$ (L = py, 1/2dppe, MeCN, THF; R = Me, Et; A = PF_6, BPh_4) (Chart 1, A), were first applied to ethylene polymerization in the absence of any cocatalyst, but the catalytic activity was not satisfied.[5] The representative catalysts based on alkylaluminium activated half-metallocene chromium complexes are $Cp^*Cr(acac)Cl/Et_3Al$ (Chart 1, B) with a catalytic activity of 4.2×10^4 g PE (mol Cr)$^{-1}$ h^{-1},[6a] as well as chromium(III) complexes bearing β-ketoiminato[6b] (Chart 1, **C**), β-diketiminato[6b] (Chart 1, D) and hydroxyindanimine[6c] ligands (Chart 1, E) with relatively high activities (1.5×10^5 g PE (mol Cr^{-1}) h^{-1}). Interestingly, with $Cp^*Cr(C_6F_5)(\eta^3\text{-}Bz)/Et_3Al$ (Bz = benzyl) (Chart 1, F) as catalyst, oligomers rather than polymers were predominantly produced with an activity of 2.1×10^5 g PE (mol Cr)$^{-1}$ h^{-1}.[7] Recently, we reported a highly efficient catalyst system based on half-metallocene type chromium(III) catalyst, $Cp^*Cr[2,4\text{-}^tBu_2\text{-}6\text{-}(CH{=}NR)\text{-}C_6H_2O]Cl/AlR'_3$ [R = ^{t}Bu, Ph, 2,6-^{i}Pr$_2$C$_6$H$_3$; R′ = Me, Et, ^{i}Bu] (Chart 1, G), for ethylene polymerization with activity up to 4.0×10^6 g PE (mol Cr)$^{-1}$ h^{-1}.[8] Indeed, only very limited alkylaluminium activated half-metallocene chromium(III) catalyst systems[8] have reached the activity level of cationic metallocene complexes of titanium and zirconium or constrained geometry chromium complexes.

Recent developments of binuclear group 4 and late transition metal complexes with MAO or fluorinated borate as activator have acted as guidelines for catalyst design in ethylene polymerization.[9,10] Binuclear metal complexes consisting of two linked active centers in a catalyst molecule usually exhibit remarkable enhancement in activity by a cooperative effect, compared with their mononuclear counterparts. For example, in a MAO activated phenoxyiminato zirconium catalyst system, the activity of a binuclear phenoxyiminato zirconium catalyst is about 8 times that of the mononuclear analogue.[9f] Herein we report the first binuclear half-metallocene chromium(III) complexes based on

---

State Key Laboratory of Fine Chemicals, College of Chemistry, Dalian University of Technology, Dalian, 116024, China. E-mail: tqxu@dlut.edu.cn, lxb-1999@163.com

† Electronic supplementary information (ESI) available. CCDC reference numbers 757579 and 821440–821442 for compounds **1**, **3**, **5** and **6**, respectively. For ESI and crystallographic data in CIF or other electronic format see DOI: 10.1039/c1dt10803d

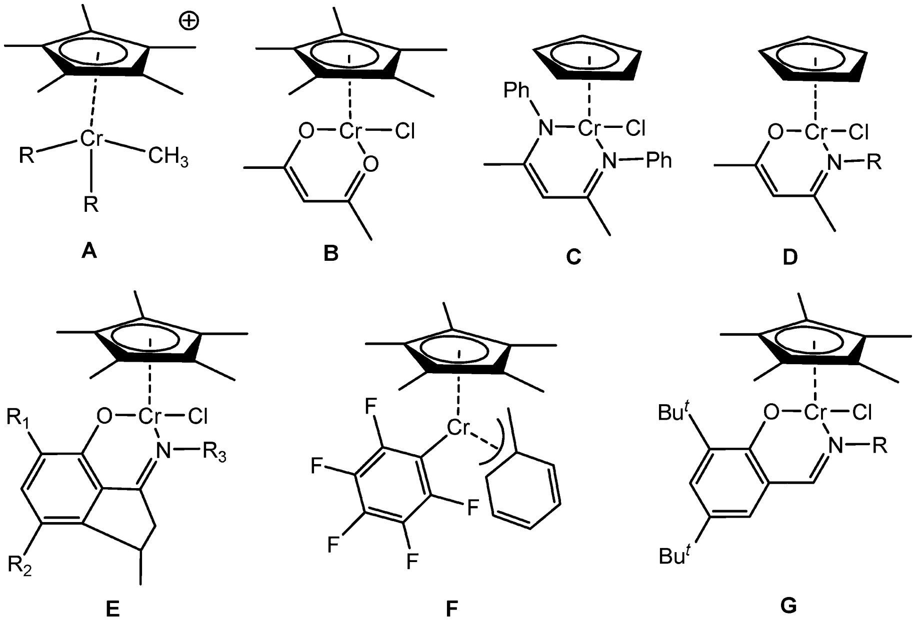

Chart 1

1,1′-binaphthyl ligands and explore their catalytic activity in the presence of a small amount of $AlMe_3$ as activator for ethylene homopolymerization.

Results and discussion

Synthesis and structural analysis

The schiff-base pro-ligands $\mathbf{L_{1-7}H}$ were synthesized in high yields by the condensation reaction of the corresponding salicylaldehyde with various amines in the presence of activated molecular sieves. The binuclear chromium complexes **1–3** were synthesized in 30–35% yield *via* the reaction of $Cp^*CrCl_2(THF)$ (THF: tetrahydrofuran) with the sodium salt of the corresponding shiff-base ligands in THF at −78 °C (Scheme 1). For a comparative purpose, mononuclear analogue complexes **4–7** were prepared through a similar procedure.

The molecular structures of complexes **1**, **3**, **5**, and **6** have been determined by a single-crystal X-ray diffraction method. X-ray structures of complexes **1**, **3**, **5**, and **6** and selected bond

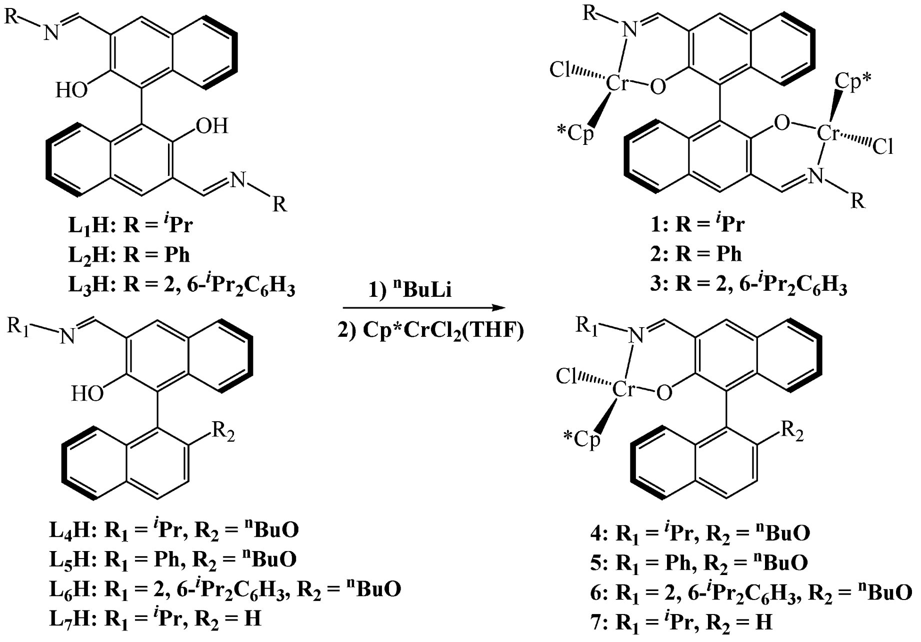

Scheme 1

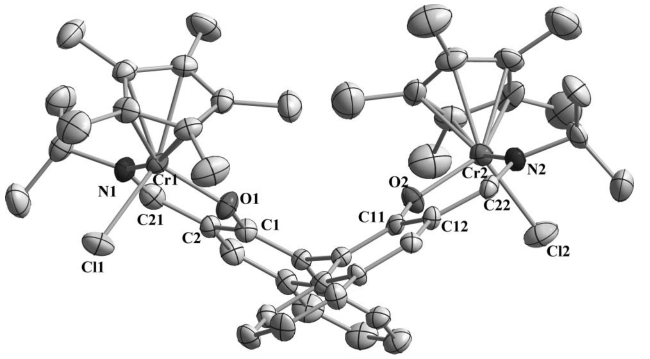

Fig. 1 Molecular structure of complex **1** (two CH_2Cl_2 solvent molecules of crystallization are omitted). Selected bond distances (Å) and angles (°): Cr(1)–O(1) 1.894(4), Cr(1)–N(1) 2.049(5), Cr(1)–Cl(1) 2.302(2), C21–N(1) 1.290(7), O(1)–C(1) 1.310(6), Cr(2)–O(2) 1.887(4), Cr(2)–N(2) 2.036(5), Cr(2)–Cl(2) 2.315(2), C22–N(2) 1.291(7), O(2)–C(11) 1.316(7); O(1)–Cr(1)–N(1) 89.13(19), O(1)–Cr(1)–Cl(1) 99.06(14), N(1)–Cr(1)–Cl(1) 89.98(15), O(2)–Cr(2)–N(2) 90.6(2), O(2)–Cr(2)–Cl(2) 98.18(14), N(2)–Cr(2)–Cl(2) 92.49(15).

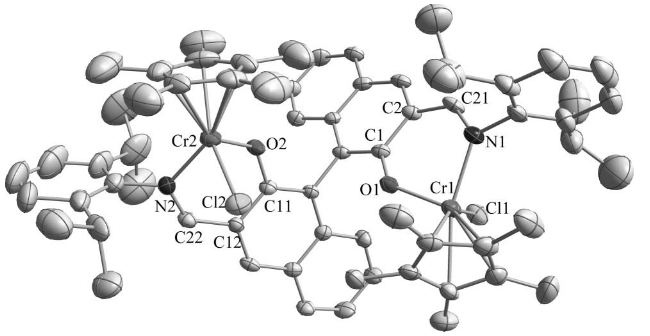

Fig. 2 Molecular structure of complex **3**. Selected bond distances (Å) and angles (°): Cr(1)–O(1) 1.905(5), Cr(1)–N(1) 2.106(6), Cr(1)–Cl(1) 2.312(3), C21–N(1) 1.288(9), O(1)–C(1) 1.299(8), Cr(2)–O(2) 1.902(5), Cr(2)–N(2) 2.102(6), Cr(2)–Cl(2) 2.292(2), C22–N(2) 1.279(8), O(2)–C(11) 1.318(7); O(1)–Cr(1)–N(1) 87.1(2), O(1)–Cr(1)–Cl(1) 96.17(17), N(1)–Cr(1)–Cl(1) 91.86(19), O(2)–Cr(2)–N(2) 85.5(2), O(2)–Cr(2)–Cl(2) 97.60(16), N(2)–Cr(2)–Cl(2) 91.61(17).

distances and angles are depicted in Fig. 1–4, respectively. In complexes **1** and **3**, two unique Cr(III) cations are joined up by binaphthol ligand to form the binuclear half-metallocene chromium molecule. Both Cr(III) cations have a pseudo-octahedral coordination environment of a three-legged piano stool. The Cr–Cp*, Cr–O, Cr–N, and Cr–Cl bond lengths in both complexes are close to those observed in some salicylaldiminato chromium complexes[11] and cyclopentadienyl chromium complexes.[5–7] Complex **1** approximates C_2 symmetry (Fig. 1). The Cr–Cl bond faces to the naphthyl ring regarding the other Cr atom. Although the two Cr sections have almost the same Cr–O, Cr–N, Cr–Cl, and Cr–C bond lengths and seemingly identical chemical environments, the coordination geometries of the two Cr atoms are slightly different. The dihedral angles between the Cp* ring and the phenoxide ring are 53.8° (Cr(1)) and 51.7°(Cr(2)). The dihedral angle between the Cp* ring and the plane through the Cr, O, and N atoms is 52.6° (Cr(1)) and 51.5°(Cr(2)). The coplanarity of the Cr(1) atom and the atoms around it is not identical with that of Cr(2). The deviations of two Cr atoms from the plane of their ligands are 0.0279 Å (Cr(1)) and 0.0015 Å (Cr(2)), respectively.

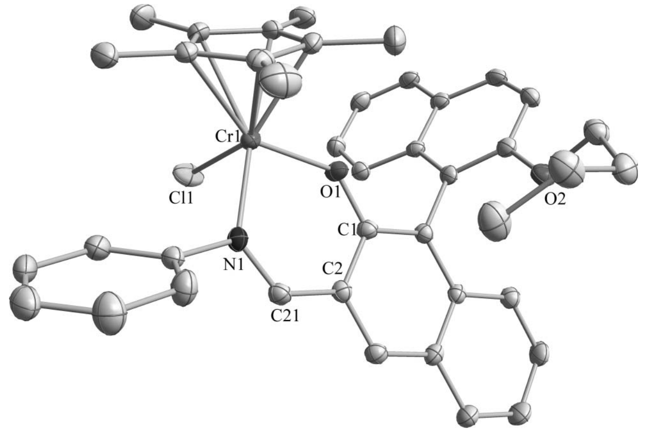

Fig. 3 Molecular structure of complex **5**. Selected bond distances (Å) and angles (°): Cr(1)–O(1) 1.9157(19), Cr(1)–N(1) 2.066(2), Cr(1)–Cl(1) 2.3147(9), C21–N(1) 1.293(3), O(1)–C(1) 1.313(3); O(1)–Cr(1)–N(1) 89.33(8), O(1)–Cr(1)–Cl(1) 96.59(7), N(1)–Cr(1)–Cl(1) 92.41(7).

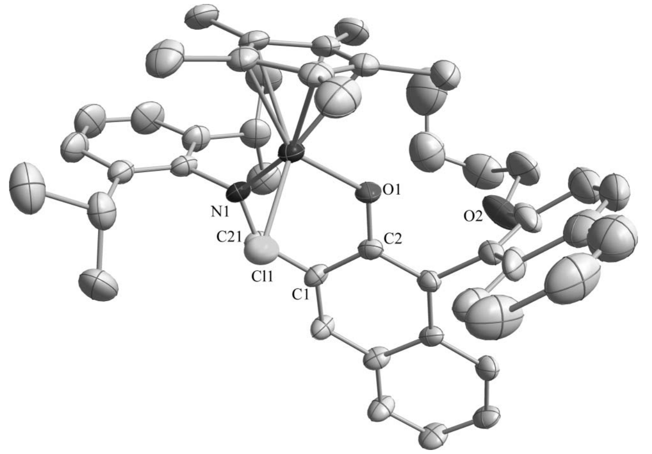

Fig. 4 Molecular structure of complex **6**. Selected bond distances (Å) and angles (°): Cr(1)–O(1) 1.915(3), Cr(1)–N(1) 2.111(4), Cr(1)–Cl(1) 2.3157(15), C21–N(1) 1.285(6), O(1)–C(1) 1.311(5); O(1)–Cr(1)–N(1) 87.72(14), O(1)–Cr(1)–Cl(1) 95.68(11), N(1)–Cr(1)–Cl(1) 91.72(11).

Interestingly, the complex **3** molecule has C_1 symmetry (Fig. 2). Similar to complex **1**, the Cr(1)–Cl(1) bond in complex **3** also faces the naphthyl ring regarding the Cr(2) atom. Whereas, the Cr(2)–Cl(2) bond faces the ring containing Cr(1), O(1), N(1), C(1), and C(21), leading to the bulky *ortho*-substituted steric group around Cr(2). The coordination geometries of the two Cr atoms are obviously different. The dihedral angles between the Cp* ring and the phenoxide ring are 84.5° (Cr(1)) and 90.6°(Cr(2)). The dihedral angles between the Cp* ring and the plane through Cr, O, and N atoms are 54.8° (Cr(1)) and 54.2°(Cr(2)). The coplanarity of the Cr(1) atom and the atoms around it is not identical to that of Cr(2). The deviations of two Cr atoms from the plane of their ligands are 0.7544 Å (Cr(1)) and 0.9116 Å (Cr(2)), respectively. Comparatively, both dihedral angles of **1** are smaller than those of **3**. The smaller dihedral angle results in more sterically opening degree around the Cr atoms of **1**,[8] which is responsible for its high activity in catalyzing ethylene polymerization (*vide infra*). The naphthol–naphthol dihedral angle of 61.9° in **1** is smaller

Table 1 Results of ethylene polymerization using precatalysts **1–7**[a]

Run	Precatalyst (μmol)	Al/Cr	AlR_3	T/°C	Yield (g)	Activity[b]	M_w[c]× 10^{-4}	M_w/M_n[c]	Tm[d] (°C)
1	1(1)	25	$AlMe_3$	20	1.57	1570	17.4	2.71	137.6
2	2(1)	25	$AlMe_3$	20	0.65	650	29.7	2.78	141.4
3	3(1)	10	$AlMe_3$	20	trace	—	—	—	—
4	3(1)	25	$AlMe_3$	20	2.87	2870	27.6	3.35	140.8
5	3(1)	50	$AlMe_3$	20	2.34	2340	22.8	3.30	139.8
6	3(1)	100	$AlMe_3$	20	2.02	2020	24.1	3.13	138.9
7	3(1)	25	$AlMe_3$	40	2.12	2120	19.6	3.37	138.7
8	3(1)	25	$AlMe_3$	60	1.56	1560	20.2	3.58	137.9
9	3(1)	25	$AlEt_3$	20	1.85	1850	20.2	3.16	138.6
10	3(1)	25	Al^iBu_3	20	1.46	1460	19.9	2.99	138.0
11	4(2)	25	$AlMe_3$	20	0.09	90	18.3	2.69	137.5
12	4(2)	50	$AlMe_3$	20	0.08	80	17.9	2.72	138.5
13	4(2)	100	$AlMe_3$	20	0.07	70	17.0	2.85	137.8
14	5(2)	25	$AlMe_3$	20	0.06	60	19.1	2.66	137.2
15	6(2)	25	$AlMe_3$	20	0.04	40	20.0	2.69	138.7
16	7(2)	25	$AlMe_3$	20	0.08	80	—	—	—

[a] Polymerization conditions: solvent, 80 mL of toluene; ethylene pressure, 5 bar; time, 30 min. [b] kg PE (mol Cr)$^{-1}$ h^{-1}. [c] Measured by GPC analysis. [d] Determined by DSC at a heating rate of 10 °C min^{-1}.

than that of 74.0° in **3**. The Cr···Cr distance of 7.504 Å in **1** is longer than that of 6.827 Å in **3**.

In the mononuclear complexes **5** and **6**, one crystallographically unique Cr(III) cation has a pseudo-octahedral coordination environment of a three-legged piano stool (Fig. 3 and 4). Both dihedral angles between the Cp* ring and the phenoxide ring and dihedral angles between the Cp* ring and the plane through Cr, O, and N atoms are 27.8° and 30.6° in complex **5**. The corresponding angles are relatively wider 53.3° and 83.2° in complex **6**. Comparatively, the dihedral angles in **6** are similar to those in Cr(1) of **3**, due to their similar coordination geometries.

Ethylene polymerization

The experimental results of ethylene polymerization with complexes **1–7** as precatalysts are summarized in Table 1. In the presence of 25 equiv. $AlMe_3$ as activator, ethylene homopolymerization using binuclear complexes **1–3** affords a high molecular weight of 1.74–2.97 × 10^5 g mol^{-1} linear polyethylene with highly catalytic activities of 0.65–2.87 × 10^6 g PE (mol Cr)$^{-1}$ h^{-1}, which are about 10–70 times that of the corresponding mononuclear analogous complexes **4–6** at the same conditions (Table 1, runs 1, 2, 4, 11, 14, and 15). To investigate if pendant ether functionality of mononuclear complexes might coordinate to the chromium center in the activated species, complex **7** without any pendant ether group was also synthesized and tested in ethylene polymerization. No distinct difference in catalytic activity for complexes **4** and **7** was observed at the same conditions (Table 1, runs 11 and 16). Indeed, the single-crystal X-ray crystallographic analyses of mononuclear complexes **5** and **6** also do not suggest the coordination of the pendant ether group to the metal ion. These results rule out the effect of the possible coordination of the pendant ether group to the chromium center during the polymerization. Thus, the superior reactivity of binuclear complexes is tentatively attributed to high local active site concentrations[9a] and good stability of the catalytically active species.[9e]

The optimal polymerization conditions were obtained for the most active complex **3** as precatalyst by varying the Al/Cr molar ratio, reaction temperature, and the kind of alkylaluminium. When the Al/Cr ratio was 10, only trace PE was found in the 30 min. The highest catalytic activity was observed in the system with an Al/Cr ratio of 25. Interestingly, a further increase in $AlMe_3$ content in the range of 25–100 equiv. has a negative influence on catalytic activity (Table 1, runs 4–6). Similar results were also observed in the catalyst systems of **4**/$AlMe_3$ (Table 1, runs 11–13), Cp*Cr(C_6F_5)(η^3-Bz)/Et_3Al[6b] and Cp*Cr[2,4-^{t}Bu-2,6-(CH═NR)-C_6H_2O]Cl/AlR_3.[8] This was tentatively explained based on the formation of a bridged heterobimetallic chromium–aluminum complex. The catalytic activities decrease with the increase of reaction temperature from 20 to 60 °C, indicating that the system was unstable at high temperature (Table 1, runs 4, 7, and 8). A similar result was also observed in the catalyst system based on the half-sandwich β-ketoiminato chromium(III) complex.[6b] The activities of these catalysts are also dependent on the AlR_3 cocatalysts and decreases in the order $AlMe_3$ > $AlEt_3$> Al^iBu_3 under the same conditions (Table 1, runs 4, 9, and 10). This may result from either a slower initiation process with the larger AlR_3 or a weak interaction between the catalyst and cocatalyst molecules, as previously reported catalyst systems.[6b,6c,8] For mononuclear chromium complexes, the catalytic activity for ethylene polymerization under similar conditions (runs 11, 14, and 15 in Table 1) is in the order of **4** > **5** > **6**. The catalytic activity of **5** with R = Ph is much higher than that of **6** with R = 2,6-^{i}Pr$_2$C$_6$H$_3$ group, which is in agreement with the order of the sterically opening degree around the chromium atom. This result is similar to the Cp*Cr[2,4-^{t}Bu-2,6-(CH═NR)-C_6H_2O]Cl/AlR_3 system.[8] On the contrary, in the catalyst systems based on binuclear chromium complexes, the enhanced steric hindrance of the R group is beneficial to improving the catalytic activity (Table 1, runs 1, 2, and 4). The highest activity of 2.87 × 10^6 g PE (mol Cr)$^{-1}$ h^{-1} was found in the catalyst system based on complex **3** with R = 2,6-^{i}Pr$_2$C$_6$H$_3$ group. We tentatively suggest that the bulky *ortho*-substituted steric groups around Cr(2) in **3** can stabilize active species during polymerization, thereby leading to an increased concentration of active species to initiate this reaction.

The gel permeation chromatography (GPC) shows that the molecular weight distributions (M_w/M_n) of the obtained polyethylenes are unimodal. The molecular weight distribution

(M_w/M_n) of polyethylenes produced by binuclear complexes **1** or **2** is close to that of the corresponding mononuclear analogue. This suggests that the two chromium centers in **1** or **2** are identical. Six typical GPC diagrams of the polyethylene samples prepared with precatalyst **1–6** are shown in Fig. 5. However, the polymers resulting from binuclear precatalyst **3** display broader molecular weight distributions (3.35) than that from its mononuclear precatalyst (2.69) under the same conditions. A possible reason is that due to the unsymmetric structure of binuclear precatalyst **3** (Fig. 2), the two Cr units are not identical. It will cause a slight difference in activity of the two active sites during the polymerization, which make a contribution to broadening the molecular weight distribution, in comparison with the scenario where there is only one active species present.[10e] ^{13}C NMR analysis on the polymer samples indicates that the polyethylenes produced by these catalysts are linear and no evidence on branch nature was observed. The melt transition temperatures (T_m) of these polymers are in the range of 137.2–141.4 °C.

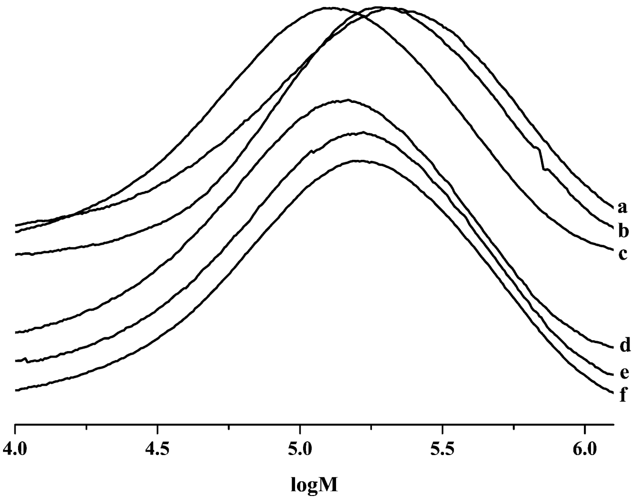

Fig. 5 The GPC traces of the polyethylene samples prepared with (a) binuclear precatalyst **3** (run 4 in Table 1), (b) binuclear precatalyst **2** (run 2 in Table 1), (c) binuclear precatalyst **1** (run 1 in Table 1), (d) mononuclear precatalyst **4** (run 11 in Table 1), (e) mononuclear precatalyst **5** (run 14 in Table 1), (f) mononuclear precatalyst **6** (run 15 in Table 1).

Magnetic properties

The solution magnetic susceptibilities of **1–7** were investigated at 300 K. Furthermore, the temperature dependence of the magnetic susceptibility of complex **3** and mononuclear analogue **6** has been investigated on crystalline samples. The magnetic susceptibilities of complexes **3** and **6** were measured in the 2.0–300.0 K temperature range under a 10 000 Oe applied field and are shown as $\chi_M T$ and $1/\chi_M$ *versus* T plots in Fig. 6 and S1.† For complex **3**, the $\chi_M T$ value at 300.0 K is 3.674 emu K mol^{-1} (5.421 μ_B), which is slightly lower than the expected value 3.75 emu K mol^{-1} (5.477 μ_B, considering $g = 2$) of two Cr(III) ions ($S = 3/2$). When decreasing the temperature, $\chi_M T$ value of **3** decreases gradually to a minimum of 2.386 emu K mol^{-1} at 2.0 K. This characteristic thermal behavior is indicative of antiferromagnetic interactions between metal spins, which also explained the low $\chi_M T$ product at room temperature. Curve fits for $1/\chi_M$ *versus* T plots of **3** with Curie–Weiss law in the range of 2.0–300.0 K get results with C = 3.692 emu cm^3 K mol^{-1} and θ = −0.84 K. The negative Weiss constant of complex **3** confirms the presence of weak antiferromagnetic interactions between spin carriers. Similar trends had also been observed in other Cr(III) complexes.[12] In dinuclear complex **3**, owing to the Cr···Cr distance (6.827 Å), only weak antiferromagnetic interactions exist between Cr(III) ions.

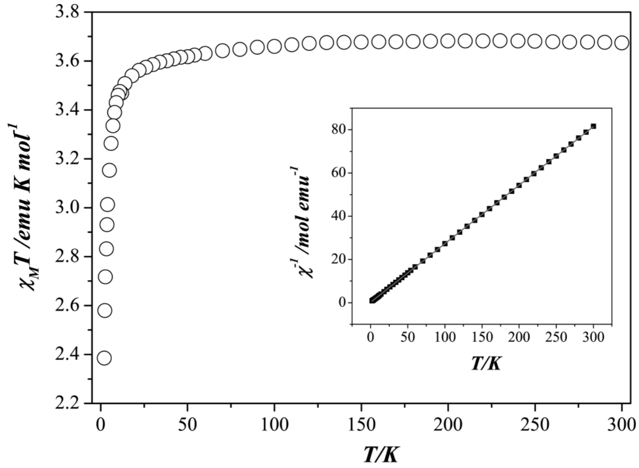

Fig. 6 The temperature dependence of reciprocal magnetic susceptibility χ_M^{-1} (square) and the product $\chi_M T$ (circle) for complex **3**.

For complex **6**, the $\chi_M T$ value at 300.0 K is 1.281 emu K mol^{-1} (3.201 μ_B), which is lower than the expected spin-only value (g = 2.0) of 1.875 emu K mol^{-1} (3.873 μ_B) for one Cr(III) ion (S = 3/2). When the temperature is lowered, the $\chi_M T$ product steadily decreases to reach a minimum of 0.865 emu K mol^{-1} at 2.0 K. The experimental data have been well fitted by the Curie–Weiss law above 2.0 K with the following Curie and Weiss constants: 1.289 emu K mol^{-1} and −0.72 K, respectively (see ESI Fig. S1†). The negative Weiss constant also confirms the presence of weak antiferromagnetic interactions between spin carriers, as was already mentioned above. In complex **6**, the interactions between Cr(III) centers are weaker than those in binuclear complex **3** according to the Weiss constant, because the Cr···Cr distance (the shortest is 8.541 Å) is significantly longer than that in complex **3**.

Conclusions

In summary, we have developed highly active binuclear half-metallocene chromium(III) catalysts for ethylene polymerization. When activated with a small amount of AlMe$_3$, these binuclear catalysts give good activities in catalyzing ethylene polymerization in comparison with their mononuclear analogues and afforded high molecular weight polymers with unimodal molecular weight distributions. The catalytic activity can be tuned by changing the R group on the imine nitrogen atom. These novel complexes represent a remarkable contribution to the limited list of half-metallocene type chromium catalysts for ethylene polymerization.

Experimental

All manipulations involving air- and/or water-sensitive compounds were carried out in a standard glove box or under dry nitrogen using standard Schlenk techniques. Toluene, terahydrofuran (THF) and hexane were distilled from sodium/benzophenone under nitrogen. Methylene chloride was distilled from CaH_2 under nitrogen.

^1H and ^{13}C NMR spectra were recorded on Varian INOVA-400 MHz type (^1H, 400 MHz) (^{13}C, 100 MHz) spectrometer. ^1H and ^{13}C NMR chemical shifts were referred to the solvent signal. A Micromass Q-Tof (Micromass, Wythenshawe, UK) mass spectrometer equipped with an orthogonal electrospray source (Zspray) operated in positive ion mode (Capillary = 2000 V, Sample cone = 20 V). Thermo-gravimetric analyses of all resulted polymers were measured on a Mettler-Toledo TGA/SDTA851e. Elemental analyses were performed on a Vario EL microanalyzer. Pro-ligands **L_1H**[13] **L_2H**[13] and **L_3H**[14] were synthesized according to the literature method.

Synthesis of 3-(CH═N^{i}Pr)-2′-^{n}BuO-2-OH-$C_{20}H_{11}$ (L_4H)

Under nitrogen, activated 4 Å molecular sieves (1.00 g), dichloromethane (10 mL) and 3-formyl-2-hydroxy-2′-butoxy-1,1′-binaphthyl[15] (1.85 g, 5 mmol) were added into a 50 mL Schlenk tube. Isopropylamine (0.29 g, 5 mmol) was added, and the mixture was stirred at room temperature. After stirring for 24 h, the reaction mixture was filtered through a pad of Celite on a medium glass fritted funnel. Then the solvent was removed *in vacuo*. The residue was purified by column chromatography on silica gel using petrol ether/ethyl acetate (5 : 1) as the mobile phase to give the afforded complex **L_4H** as a bright yellow solid (1.64 g, 80%). ^1H NMR (400 MHz, $CDCl_3$) δ 13.33 (s, 1H), 8.62 (s, 1H), 7.94 (d, J = 9.2 Hz, 1H), 7.90 (s, 1H), 7.86 (d, J = 2.8 Hz, 1H), 7.84 (s,1H), 7.44 (d, J = 8.8 Hz, 1H), 7.25–7.33 (m, 6H), 7.12 (d, J = 8.0 Hz, 2H), 3.93–4.04 (m, 2H), 3.60 (hept, 1H), 1.35–1.43 (m, 2H), 1.27 (d, J = 4.0 Hz, 6H), 0.93–1.00 (m, 2H), 0.61 (t, 3H). ^{13}C NMR (100 MHz, $CDCl_3$) δ 162.3, 154.8, 154.7, 135.5, 134.0, 132.6, 129.6, 129.5, 128.6, 128.1, 127.9, 127.4, 126.4, 125.4, 125.1, 123.7, 123.1, 121.0, 120.0, 117.5, 116.2, 69.6, 60.5, 31.4, 24.2, 18.8, 13.7. HRMS (m/z) Calcd. for $[C_{28}H_{30}NO_2]^+$: 412.2277, found: 412.2293.

Synthesis of 3-(CH═NPh)-2′-^{n}BuO-2-OH-$C_{20}H_{11}$ (L_5H)

The pro-ligand **L_5H** was prepared as a similar procedure of **L_4H**. ^1H NMR (400 MHz, $CDCl_3$) δ 13.03 (s, 1H), 8.92 (s, 1H), 8.10 (s, 1H), 7.98 (d, J = 8.8 Hz, 1H), 7.87–7.91 (m, 2H), 7.47 (d, J = 8.8 Hz, 1H), 7.24–7.35 (m, 9H), 7.17 (d, J = 7.6 Hz, 4H), 4.01–4.09 (m, 2H), 1.37–1.45 (m, 2H), 0.94–1.01 (m, 2H), 0.61 (t, J = 7.2 Hz, 3H). ^{13}C NMR (100 MHz, $CDCl_3$) δ 162.6, 154.8, 154.4, 148.3, 136.1, 134.4, 134.0, 129.7, 129.6, 129.5, 128.8, 128.4, 128.2, 127.6, 127.2, 126.5, 125.3, 125.2, 123.7, 123.4, 121.2, 121.1, 119.7, 118.0, 116.1, 69.6, 31.4, 18.8, 13.6. HRMS (m/z) Calcd. for $[C_{31}H_{28}NO_2]^+$: 446.2120, found: 446.2141.

Synthesis of 3-(CH═N-2,6-^{i}Pr$_2$-C_6H_3)-2′-^{n}BuO-2-OH-$C_{20}H_{11}$ (L_6H)

The pro-ligand **L_6H** was prepared as a similar procedure of **L_4H**. ^1H NMR (400 MHz, $CDCl_3$) δ 12.56 (s, 1H), 8.56 (s, 1H), 8.02 (s, 1H), 8.01 (d, J = 1.2 Hz, 1H), 7.87–7.91 (m, 2H), 7.48 (d, J = 8.8 Hz, 1H), 7.28–7.36 (m, 5H), 7.17–7.20 (m, 4H), 4.01–4.09 (m, 2H), 3.04 (hept, 2H), 1.43–1.51 (m, 2H), 1.18 (d, J = 4.0 Hz, 12H), 1.03–1.11 (m, 2H), 0.65 (t, 3H). ^{13}C NMR (100 MHz, $CDCl_3$) δ 167.0, 154.9, 154.6, 146.6, 138.8, 136.2, 134.4, 134.0, 129.8, 129.6, 128.8, 128.6, 128.2, 127.5, 126.5, 125.6, 125.4, 125.3, 123.7, 123.5, 123.4, 120.6, 119.6, 118.2, 116.2, 69.7, 31.5, 28.2, 23.8, 23.7, 18.8, 13.7. HRMS (m/z) Calcd. for $[C_{37}H_{40}NO_2]^+$: 530.3059, found: 530.3045.

Synthesis of 2-methoxymethoxy-1,1′-binaphthyl

To a 100 mL three-necked flask equipped with a pressure-funnel, a rubber-stopper and a magnetic stir bar, THF (30 mL) and NaH (0.12 g) were added. When the mixture was cooled down to 0 °C, a solution of 2-hydroxy-1,1′-binaphthyl[16] (1.35 g, 5 mmol) in 10 mL THF was added dropwise. After 1 h, 1.2 mL methoxymethyl chloride (MOMCl) was added by a syringe. The reaction was then continued for another 4 h at room temperature and then quenched with 100 mL water. This mixture was extracted three times with 50 mL ethyl acetate. The combined organic phase was washed with water and brine, and dried over $MgSO_4$. Then the solvent was removed *in vacuo*. The residue was purified by column chromatography on silica gel using petrol ether/ethyl acetate (1 : 1, v/v) as the mobile phase to give the afforded compound as a white solid (1.34 g, 85%). ^1H NMR (400 MHz, $CDCl_3$) δ 7.93–7.96 (m, 3H), 7.87 (d, 1H, J = 8.4 Hz), 7.61 (t, J = 7.2 Hz, 1H), 7.56 (d, J = 7.2 Hz 1H), 7.44–7.48 (m, 2H), 7.34–7.37 (m, 2H), 7.28 (d, J = 6.8 Hz, 1H), 7.22 (d, J = 4.0 Hz, 1H), 7.17 (d, J = 4.0 Hz, 1H), 5.02 (s, 2H), 3.14 (s, 3H).

Synthesis of 3-formyl-2-methoxymethoxy-1,1′-binaphthyl

To a solution of 2-methoxymethoxy-1,1′-binaphthyl (0.79 g, 2.5 mmol) and TMEDA (0.58 g, 5 mmol) in THF (20 mL), 1.6 mL ^{n}BuLi (1.6 M in hexane) was added at −78 °C under nitrogen. The mixture was warmed up to 0 °C and stirred for 30 min and then cooled down to −78 °C. A solution of DMF (0.37 g, 5 mmol) in THF (5 mL) was added dropwise. This reaction solution was warmed up to 0 °C and stirred for 2 h. The obtained solution was quenched with 50 mL saturated NH_4Cl solution. After separating the organic layer, the water layer was extracted with ethyl ether. The combined organic layer was washed with brine, and dried over $MgSO_4$. After removing the organic solvent, the residue was treated with a flash chromatography using the petroleum ether and ethyl acetate as eluent (5 : 1, v/v) to give the afforded compound as a white solid (0.64 g, 75%). ^1H NMR (400 MHz, $CDCl_3$) δ 10.57 (s, 1H), 8.57 (s, 1H), 8.04 (d, J = 8.0 Hz, 1H), 7.95–8.01 (m, 3H), 7.63 (t, J = 8.0 Hz, 1H), 7.46–7.53 (m, 3H), 7.33–7.39 (m, 3H), 4.64 (d, J = 1.6 Hz, 2H), 2.92 (s, 3H).

Synthesis of 3-formyl-2-hydroxy-1,1′-binaphthyl

To a solution of 3-formyl-2-methoxymethoxy-1,1′-binaphthyl (0.51 g, 1.50 mmol) in THF (10 mL), 10 mL concentrated HCl was added dropwise at 0 °C. This mixture was then stirred for 3 h at room temperature and then extracted with ethyl acetate. The obtained solution was washed with water, and dried with Na_2SO_4. After evaporating the solvent, the product was obtained as a yellow solid (0.43 g, 96%). ^1H NMR (400 MHz, $CDCl_3$) δ 10.49 (s, 1H), 10.19 (s, 1H), 8.31 (s, 1H), 7.95–8.00 (m, 3H), 7.64 (d, J = 8.0 Hz, 1H), 7.46–7.53 (m, 3H), 7.25–7.38 (m, 4H), 7.20–7.22 (m, 1H).

Synthesis of 3-(CH═N^{i}Pr)-2-OH-$C_{20}H_{11}$ (L_7H)

Under nitrogen, activated molecular sieves (4 Å, 0.5 g), dichloromethane (10 mL) and 3-formyl-2-hydroxy-1,1′-binaphthyl

(0.29 g, 1 mmol) were added into a 50 mL Schlenk tube. Isopropylamine (0.12 g, 2 mmol) was added, and the mixture was stirred at room temperature. After stirring for 10 h, the reaction mixture was filtered through a pad of Celite on a medium glass fritted funnel. The solvent was removed in vacuo. The residue was purified by column chromatography on silica gel using petrol ether/ethyl acetate (5 : 1, *v*/*v*) as the mobile phase to give the afforded complex **L_7H** as a pale yellow solid (0.31 g, 91%). ^1H NMR (400 MHz, $CDCl_3$) δ 13.51 (s, 1H), 8.62 (s, 1H), 7.92–7.97 (m, 3H), 7.86 (d, 1H), 7.63 (t, J = 7.6 Hz, 1H), 7.40–7.50 (m, 3H), 7.26–7.30 (m, 3H), 7.15 (d, J = 4.0 Hz, 1H), 3.60 (hept, 1H), 1.35–1.43 (m, 2H), 1.27 (d, J = 4.0 Hz, 6H). ^{13}C NMR (100 MHz, $CDCl_3$) δ 162.1, 154.6, 154.5, 135.4, 134.1, 134.0, 132.8, 132.7, 128.6, 128.4, 128.1, 128.0, 127.2, 126.1, 126.0, 125.8, 125.7, 125.2, 123.3, 121.0, 120.9, 60.5, 24.2. HRMS (*m*/*z*) Calcd. for $[C_{24}H_{22}NO]^+$: 340.1701, found: 340.1686.

Synthesis of {Cp*[3-(CH=N^{i}Pr)-2-O-$C_{10}H_5$]CrCl}$_2$ (1)

Under nitrogen, a solution of pro-ligand **L_1H** (0.53 g, 1.25 mmol) in THF was added to a mixture NaH (0.07 g, 2.92 mmol) in THF (10 mL) at −78 °C. The reaction mixture was allowed to warm to room temperature and stirred for 2 h, and then the reaction mixture was filtered through a pad of Celite on a medium glass fritted funnel. The filtrate was added at −78 °C to a solution of Cp*$CrCl_2$(THF) which was prepared by the reaction of $CrCl_3(THF)_3$ (0.94 g, 2.50 mmol) with Cp*Li (0.36 g, 2.50 mmol) in THF (30 mL). The resulting mixture was allowed to warm to room temperature and stirred for 15 h, during which time the color changed from blue to purple. The solvent was removed under vacuum, and the residue was extracted with CH_2Cl_2 (20 mL) and filtered. The filtrate was concentrated to 5 mL and mixed with hexane (50 mL). Cooling to –30 °C afforded purple crystals of complex **1** after several days (0.37 g, 0.43 mmol, 34%). HRMS (*m*/*z*) Calcd. for $[C_{48}H_{56}N_2O_2ClCr_2]^+$: 831.2841, found: 831.2809. Anal. Calcd. for $C_{48}H_{56}N_2O_2Cl_2Cr_2$ (%): C 66.43; H 6.50; N 3.23. Found: C 66.51; H 6.40; N 3.27. UV/vis (dichloromethane): 243, 316 487 nm. Magnetic measurement: μ_{eff} (solution in benzene, 300 K) = 5.39 μ_B.

Synthesis of {Cp*[3-(CH=NPh)-2-*O*-$C_{10}H_5$]CrCl}$_2$ (2)

Complex **2** was synthesized in the same way as described above for the synthesis of complex **1** with proligand **L_2H** (0.62 g, 1.25 mmol) as starting material. Pure complex **2** (0.35 g, 0.37 mmol, 30%) was obtained as purple crystals. HRMS (*m*/*z*) Calcd. for $[C_{54}H_{52}N_2O_2ClCr_2]^+$: 899.2528, found: 899.2551. Anal. Calcd. for $C_{54}H_{52}N_2O_2Cl_2Cr_2$ (%): C 69.30; H 5.60; N 2.99. Found: C 69.38; H 5.71; N 3.05. UV/vis (dichloromethane): 244, 315, 487 nm. Magnetic measurement: μ_{eff} (solution in benzene, 300 K) = 5.41 μ_B.

Synthesis of {Cp*[3-(CH=N-2,6-^{i}Pr$_2$-C_6H_3)-2-O-$C_{10}H_5$]CrCl}$_2$ (3)

Complex **3** was synthesized in the same way as described above for the synthesis of complex **1** with pro-ligand **L_3H** (0.83 g, 1.25 mmol) as starting material. Pure complex **3** (0.48 g, 0.44 mmol, 35%) was obtained as purple crystals. HRMS (*m*/*z*) Calcd. for $[C_{66}H_{76}N_2O_2ClCr_2]^+$: 1067.4406, found: 1067.4385. Anal. Calcd. for $C_{66}H_{76}N_2O_2Cl_2Cr_2$ (%): C 71.79; H 6.94; N 2.54. Found: C 71.70; H 7.02; N 2.49. UV/vis (dichloromethane): 243, 315, 487 nm. Magnetic measurement: μ_{eff} (solution in benzene, 300 K) = 5.42 μ_B.

Synthesis of Cp*[3-(CH=N^{i}Pr)-2′-^{n}BuO-2-O-$C_{20}H_{11}$]CrCl (4)

Complex **4** was synthesized in the same way as described above for the synthesis of complex **1** with pro-ligand **L_4H** (1.03 g, 2.50 mmol) as starting material. Pure complex **4** (0.81 g, 1.28 mmol, 51%) was obtained as purple crystals. HRMS (*m*/*z*) Calcd. for $[C_{38}H_{43}NO_2Cr]^+$: 597.2699, found: 597.2678. Anal. Calcd. for $C_{38}H_{43}NO_2ClCr$ (%): C 72.08; H 6.84; N 2.21. Found: C 72.14; H 6.85; N 2.25. UV/vis (dichloromethane): 244, 315, 466 nm. Magnetic measurement: μ_{eff} (solution in benzene, 300 K) = 3.32 μ_B.

Synthesis of Cp*[3-(CH=NPh)-2′-^{n}BuO-2-*O*-$C_{20}H_{11}$]CrCl (5)

Complex **5** was synthesized in the same way as described above for the synthesis of complex **1** with pro-ligand **L_5H** (1.11 g, 2.50 mmol) as starting material. Pure complex **5** (0.75 g, 1.13 mmol, 45%) was obtained as purple crystals. HRMS (*m*/*z*) Calcd. for $[C_{41}H_{41}NO_2Cr]^+$: 631.2542, found: 631.2518. Anal. Calcd. for $C_{41}H_{41}NO_2ClCr$ (%): C 73.80; H 6.19; N 2.10. Found: C 73.82; H 7.23; N 2.04. UV/vis (dichloromethane): 243, 314, 469 nm. Magnetic measurement: μ_{eff} (solution in benzene, 300 K) = 3.36 μ_B.

Synthesis of Cp*[3-(CH=N-2,6-^{i}Pr$_2$-C_6H_3)-2′-^{n}BuO-2-O-$C_{20}H_{11}$]-CrCl (6)

Complex **6** was synthesized in the same way as described above for the synthesis of complex **1** with pro-ligand **L_6H** (1.32 g, 2.50 mmol) as starting material. Pure complex **6** (0.56 g, 0.75 mmol, 30%) was obtained as purple crystals. HRMS (*m*/*z*) Calcd. for $[C_{47}H_{53}NO_2Cr]^+$: 715.3481, found: 715.3457. Anal. Calcd. for $C_{47}H_{53}NO_2ClCr$ (%): C 75.13; H 7.11; N 1.86. Found: C 75.19; H 7.19; N 1.80. UV/vis (dichloromethane): 244, 315, 467 nm. Magnetic measurement: μ_{eff} (solution in benzene, 300 K) = 3.20 μ_B.

Synthesis of Cp*[3-(CH=N-2,6-^{i}Pr$_2$-C_6H_3)-2-O-$C_{20}H_{11}$]CrCl (7)

Complex **7** was synthesized in the same way as described above for the synthesis of complex **1** with pro-ligand **L_7H** (0.85 g, 2.50 mmol) as starting material. Pure complex **7** (0.61 g, 1.15 mmol, 46%) was obtained as purple crystals. HRMS (*m*/*z*) Calcd. for $[C_{34}H_{35}NOCr]^+$: 525.2124, found: 525.2132. Anal. Calcd. for $C_{34}H_{35}NOClCr$ (%): C 72.78; H 6.29; N 2.50. Found: C 72.83; H 6.23; N 2.54. UV/vis (dichloromethane): 249, 315, 469 nm. Magnetic measurement: μ_{eff} (solution in benzene, 300 K) = 3.38 μ_B.

Ethylene polymerizations

A dry 250 mL steel autoclave with a magnetic stirrer was charged with 80 mL of toluene, and saturated with ethylene (1.0 bar) at 20 °C. The polymerization reaction was started by injection of a mixture of $AlMe_3$ and a catalyst in toluene (10 mL). The vessel was immediately repressurized to the required pressure with ethylene and the pressure was kept by continuous feeding of ethylene. After 30 min, the polymerization was quenched by injecting acidified

Table 2 Crystal data and structural refinement details for complexes **1**, **3**, **5**, and **6**

	1	**3**	**5**	**6**
Mol formula	$C_{50}H_{60}Cl_6Cr_2N_2O_2$	$C_{66}H_{76}Cl_2Cr_2N_2O_2$	$C_{41}H_{41}ClCrNO_2$	$C_{47}H_{53}ClCrNO_2$
Mol wt	1037.70	1104.19	667.20	751.35
Cryst system	Monoclinic	Monoclinic	Triclinic	Monoclinic
Space group	$P2_1/c$	$P2_1/c$	$P\bar{1}$	$P2_1/c$
a/Å	16.312(4)	18.076(5)	8.6023(7)	11.6666(16)
b/Å	12.288(4)	18.047(5)	12.9253(11)	20.495(3)
c/Å	29.792(6)	23.103(4)	16.4342(14)	17.050(2)
α (°)	90	90.00	69.8440(10)	90.00
β (°)	120.392(10)	125.714(14)	83.356(2)	92.581(2)
γ (°)	90	90.00	79.470(2)	90.00
V/Å^3	5151(2)	6119(3)	1683.7(2)	4072.6(9)
Z	4	4	2	4
F(000)	2160	2336	702	1596
D_c (g cm^{-3})	1.338	1.199	1.316	1.225
μ/mm^{-1}	0.772	0.485	0.456	0.385
R_{int}	0.1294	0.1491	0.0229	0.0712
$R_1(I > 2\delta)$	0.0715	0.0940	0.0513	0.0731
WR_2 (I>2δ)	0.1480	0.1695	0.1202	0.1623
GOF	0.995	1.024	1.021	1.056

methanol [HCl (3 M)/methanol = 1 : 1], and the polymer was collected by filtration, washed with water, methanol, and dried at 60 °C *in vacuo* to a constant weight.

Crystal structure determination

Single crystals of complexes **1**, **3**, **5**, and **6** for X-ray structural analysis were obtained from a solution of $CH_2Cl_2/^n$hexane. Diffraction data was collected at 293 K (for **1** and **5**) or 200 K (for **3** and **6**) on a Bruker SMART-CCD diffractometer using graphite-monochromated Mo-Kα radiation (λ = 0.71073 Å). The structure was solved by direct methods[17] and refined by full-matrix least-squares on F^2. All non-hydrogen atoms were refined anisotropically, and the hydrogen atoms were included in an idealized position. All calculations were performed using the SHELXTL[18] crystallographic software packages. Details of the crystal data, data collections, and structure refinements are summarized in Table 2.

Acknowledgements

This work was supported by the National Natural Science Foundation of China (No. 20804006) and Specialized Research Fund for the Doctoral Program of Higher Education (No. 200801411015), and the Fundamental Research Funds for the Central Universities (DUT11LK24). X.-B. Lu gratefully acknowledges the Outstanding Yong Scientist Foundation of NSFC (Grant 20625414). The authors also thank Dr Haiyan An for her great help in describing magnetic properties of various chromium complexes and single-crystal X-ray crystallographic analysis.

References

1 (*a*) W. Kaminsky, K. Kulper and H. H. Brintzinger, *Angew. Chem., Int. Ed. Engl.*, 1985, **24**, 507; (*b*) J. A. Ewen, *J. Am. Chem. Soc.*, 1984, **106**, 6355.

2 (*a*) J. A. Ewen, R. L. Jones, A. Razavi and J. D. Ferrara, *J. Am. Chem. Soc.*, 1988, **110**, 6255; (*b*) H. G. Alt and E. Samuel, *Chem. Soc. Rev.*, 1998, **27**, 323.

3 (*a*) C. Bae, J. F. Hartwig, H. Chung, N. K. Harris, K. A. Switek and M. A. Hillmyer, *Angew. Chem., Int. Ed.*, 2005, **44**, 6410; (*b*) A. L. Mckniht and R. M. Waymouth, *Chem. Rev.*, 1998, **98**, 2587.

4 (*a*) N. Ishihara, T. Seimiya, M. Kuramoto and M. Uoi, *Macromolecules*, 1986, **19**, 2464; (*b*) G. Xu and D. Chien, *Macromolecules*, 2000, **33**, 2825; (*c*) Y. Luo, J. Baldamus and Z. Hou, *J. Am. Chem. Soc.*, 2004, **126**, 13910; (*d*) K. Nomura, N. Naga, M. Miki, K. Yanagi and A. Imai, *Organometallics*, 1998, **17**, 2152.

5 (*a*) B. J. Thomas and K. H. Theopold, *J. Am. Chem. Soc.*, 1988, **110**, 5902; (*b*) B. J. Thomas, S. K. Noh, G. K. Schulte, S. C. Sendlinger and K. H. Theopold, *J. Am. Chem. Soc.*, 1991, **113**, 893.

6 (*a*) O. Heinemann, P. W. Jolly, C. Kruger and G. P. J. Verhovnik, *J. Organomet. Chem.*, 1998, **553**, 477; (*b*) Y. Huang, W. Yu and G. Jin, *Dalton Trans.*, 2009, 767; (*c*) Y. Huang, W. Yu and G. Jin, *Organometallics*, 2009, **28**, 4170.

7 G. Mani and F. P. Gabbai, *Angew. Chem., Int. Ed.*, 2004, **43**, 2263.

8 T. Xu, Y. Mu, W. Gao, J. Ni, L. Ye and Y. Tao, *J. Am. Chem. Soc.*, 2007, **129**, 2236.

9 (*a*) L. Li, M. V. Metz, H. Li, M. Chen, T. J. Marks, L. Liable-Sands and A. L. Rheingold, *J. Am. Chem. Soc.*, 2002, **124**, 12725; (*b*) H. Li, L. Li, T. J. Marks, L. Liable-Sands and A. L. Rheingold, *J. Am. Chem. Soc.*, 2003, **125**, 10788; (*c*) N. Guo, L. Li and T. J. Marks, *J. Am. Chem. Soc.*, 2004, **126**, 6542; (*d*) A. Motta, I. L. Fragala and T. J. Marks, *J. Am. Chem. Soc.*, 2007, **129**, 7327; (*e*) N. Guo, C. Stern and T. J. Marks, *J. Am. Chem. Soc.*, 2008, **130**, 2246; (*f*) M. R. Salata and T. J. Marks, *J. Am. Chem. Soc.*, 2008, **130**, 12; (*g*) H. Li, C. L. Stern and T. J. Marks, *Macromolecules*, 2005, **38**, 9015; (*h*) M. H. Lee, S. K. Kim and Y. Do, *Organometallics*, 2005, **24**, 3618; (*i*) S. K. Noh, W. Jung, H. Oh, Y. R. Lee and W. S. Lyoo, *J. Organomet. Chem.*, 2006, **691**, 5000.

10 (*a*) M. R. Salata and T. J. Marks, *J. Am. Chem. Soc.*, 2008, **130**, 12; (*b*) B. A. Rodriguez, M. Delferro and T. J. Marks, *J. Am. Chem. Soc.*, 2009, **131**, 5902; (*c*) M. R. Salata and T. J. Marks, *Macromolecules*, 2009, **42**, 1920; (*d*) T. Hu, Y. Li, J Liu and Y. Li, *Organometallics*, 2007, **26**, 2609; (*e*) T. Hu, L. Tang, X. Li, Y. Li and N. Hu, *Organometallics*, 2005, **24**, 2628.

11 V. C. Gibson, S. Mastroianni, C. Newton, C. Redshaw, G. A. Solan, A. J. P. White and D. J. Williams, *J. Chem. Soc., Dalton Trans.*, 2000, 1969.

12 (*a*) S. Y. Jie, R. Pattacini, G. Rogez, C. Loose, J. Kortusd and P. Braunstein, *Dalton Trans.*, 2009, 97–105; (*b*) M. Salidu, F. Artizzu, P. Deplano, M. L. Mercuri, L. Pilia, A. Serpe, L. Marchiò, G. Concasc and F. Congiuc, *Dalton Trans.*, 2009, 557.

13 H. Brunner and J. Goldbrunner, *Chem. Ber.*, 1989, **122**, 2005.

14 T. Hu, Y. Li, Y. Li and N. Hu, *J. Mol. Catal. A: Chem.*, 2006, **253**, 155.

15 L. Jin, Y. Huang, H. Jing, T. Chang and P. Yan, *Tetrahedron: Asymmetry*, 2008, **19**, 1947.

16 P. Wawrzyniak and J. Heinicke, *Tetrahedron Lett.*, 2006, **47**, 8921.

17 *SHELXTL*PC Siemens Analytical X-ray Instruments: Madison, WI, 1993.

18 G. M. Sheldrick, *SHELXTL Structure Determination Programs*, Version 6.12; PC Siemens Analytical Systems: Madison, WI, 1994.